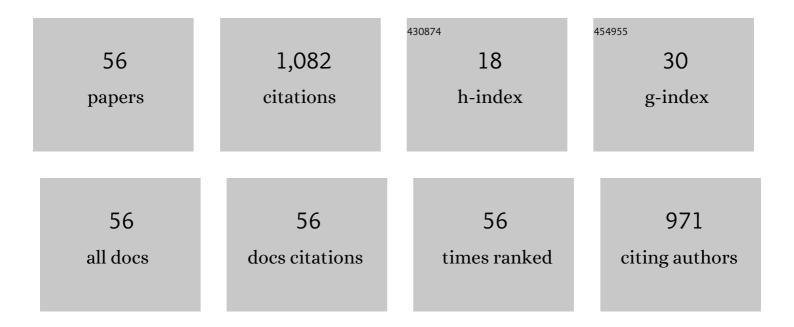
## Abhishek Ghosh

List of Publications by Year in descending order

Source: https://exaly.com/author-pdf/1840809/publications.pdf Version: 2024-02-01



#	Article	IF	CITATIONS
1	Bilateral Tunnelized FAMM Islanded Flap for Reconstruction of Composite Defect of Tongue and Floor of Mouth: A Case Report. Journal of Maxillofacial and Oral Surgery, 2024, 23, 49-52.	1.4	0
2	Sensitive and selective CO2 gas sensor based on CuO/ZnO bilayer thin-film architecture. Journal of Alloys and Compounds, 2022, 903, 163871.	5.5	39
3	MEMS GC Column Performance for Analyzing Organics and Biological Molecules for Future Landed Planetary Missions. Frontiers in Astronomy and Space Sciences, 2022, 9, .	2.8	5
4	Flow behavior and strain rate sensitivity assessment of γ and γʹ phases in Co–Al–W-based superalloy using experimental and computational approaches. Journal of Materials Research and Technology, 2022, 18, 4617-4630.	5.8	5
5	Integration of RS-GIS with Frequency Ratio, Fuzzy Logic, Logistic Regression and Decision Tree Models for Flood Susceptibility Prediction in Lower Gangetic Plain: A Study on Malda District of West Bengal, India. Journal of the Indian Society of Remote Sensing, 2022, 50, 1725-1745.	2.4	13
6	Sensitivity analysis of multilayered C-axis inclined zigzag zinc oxide thin-film bulk acoustic resonators for CO <sub>2</sub> concentration monitoring. Mechanics of Advanced Materials and Structures, 2021, 28, 699-708.	2.6	5
7	Influence of temperature on microstructure, crystallographic texture and mechanical properties of EN AW 6016 alloy during plane strain compression. Materials Today Communications, 2021, 26, 101808.	1.9	7
8	Flood Severity assessment of the coastal tract situated between Muriganga and Saptamukhi estuaries of Sundarban delta of India using Frequency Ratio (FR), Fuzzy Logic (FL), Logistic Regression (LR) and Random Forest (RF) models. Regional Studies in Marine Science, 2021, 42, 101624.	0.7	20
9	Impact of Climatic Variations on Drug-induced Skin Reactions in Two Different Regions of India. Current Drug Safety, 2021, 16, 90-96.	0.6	2
10	3D FEM simulation of Al-Zn-Mg-Cu alloy during multi-pass ECAP with varying processing routes. Materials Today Communications, 2021, 26, 102112.	1.9	13
11	Integrated microfluidic helium discharge photoionization detectors. Sensors and Actuators B: Chemical, 2021, 332, 129504.	7.8	9
12	Soil erosion susceptibility assessment using logistic regression, decision tree and random forest: study on the Mayurakshi river basin of Eastern India. Environmental Earth Sciences, 2021, 80, 1.	2.7	50
13	High-Sensitivity Micro-Gas Chromatograph–Photoionization Detector for Trace Vapor Detection. ACS Sensors, 2021, 6, 2348-2355.	7.8	30
14	Effect of beam current on the microstructure, crystallographic texture and mechanical properties of electron beam welded high purity niobium. Materials Characterization, 2021, 179, 111318.	4.4	10
15	Phase transformation and dispersoid evolution for Al-Zn-Mg-Cu alloy containing Sn during homogenisation. Journal of Materials Research and Technology, 2020, 9, 1-12.	5.8	40
16	O to T Flap for Central Forehead Defect Reconstruction. Journal of Maxillofacial and Oral Surgery, 2020, 19, 523-526.	1.4	3
17	Experimental Coupling of a MEMS Gas Chromatograph and a Mass Spectrometer for Organic Analysis in Space Environments. ACS Earth and Space Chemistry, 2020, 4, 1718-1729.	2.7	8
18	Selective H2 sensing using lanthanum doped zinc oxide thin film: A study of temperature dependence H2 sensing effect on carrier reversal activity. Journal of Applied Physics, 2020, 128, .	2.5	9

Авнізнек Снозн

#	Article	IF	CITATIONS
19	Parametric optimization of WEDM for EN AW 7075 alloy processed by ECAP. Materials Today: Proceedings, 2020, 33, 5279-5283.	1.8	2
20	Investigation of phase evolution of Al–Si–Mg coating on hot dipped interstitial-free steel. Results in Materials, 2020, 6, 100078.	1.8	8
21	Development of ultrafine grained Al–Zn–Mg–Cu alloy by equal channel angular pressing: microstructure, texture and mechanical properties. Archives of Civil and Mechanical Engineering, 2020, 20, 1.	3.8	25
22	Multilayered and Chemiresistive Thin and Thick Film Gas Sensors for Air Quality Monitoring. , 2020, , .		8
23	Miniaturized langasite MEMS micro-cantilever beam structured resonator for high temperature gas sensing. Smart Materials and Structures, 2020, 29, 055002.	3.5	12
24	Effect of heat treatment and severe plastic deformation on microstructure and texture evolution of 7075 alloy. Materials Today: Proceedings, 2020, 33, 5239-5242.	1.8	7
25	Langasite-based surface acoustic wave resonator for acetone vapor sensing. Smart Materials and Structures, 2020, 29, 015039.	3.5	11
26	Monitoring estuarine morphodynamics through quantitative techniques and GIS: A Case study in Sagar Island, India. Journal of Coastal Conservation, 2019, 23, 133-148.	1.6	6
27	High temperature CO2 sensing and its cross-sensitivity towards H2 and CO gas using calcium doped ZnO thin film coated langasite SAW sensor. Sensors and Actuators B: Chemical, 2019, 301, 126958.	7.8	71
28	CO <sub>2</sub> Sensing Behavior of Calcium-Doped ZnO Thin Film: A Study To Address the Cross-Sensitivity of CO <sub>2</sub> in H <sub>2</sub> and CO Environment. Langmuir, 2019, 35, 10267-10275.	3.5	27
29	Highâ€Temperature Gas Sensors for Harsh Environment Applications: A Review. Clean - Soil, Air, Water, 2019, 47, 1800491.	1.1	39
30	Influence of homogenisation time on evolution of eutectic phases, dispersoid behaviour and crystallographic texture for Al–Zn–Mg–Cu–Ag alloy. Journal of Alloys and Compounds, 2019, 802, 276-289.	5.5	42
31	Catalytic oxidation and selective sensing of carbon monoxide for sense and shoot device using ZnO–CuO hybrids. Materialia, 2019, 5, 100177.	2.7	8
32	CO2 sensing characteristics of SAW sensor operated at high temperature. , 2019, , .		0
33	Microstructure and texture development of 7075 alloy during homogenisation. Philosophical Magazine, 2018, 98, 1470-1490.	1.6	40
34	Multi-layered zinc oxide-graphene composite thin films for selective nitrogen dioxide sensing. Journal of Applied Physics, 2018, 123, .	2.5	10
35	Understanding the evolution of microstructural features in the in-situ intermetallic phase reinforced Al/Al 3 Ti nanocomposite. Materials Today: Proceedings, 2018, 5, 10118-10130.	1.8	11
36	Spatiotemporal changes of geomorphic environment in the Muriganga–Saptamukhi estuarine interfluve of Indian Sundarban in the context of climate change: a case study. Environment, Development and Sustainability, 2018, 20, 1153-1172.	5.0	2

Авнізнек Снозн

#	Article	IF	CITATIONS
37	Tensile and impact behaviour of thermo mechanically treated and micro-alloyed medium carbon steel bar. Construction and Building Materials, 2018, 192, 657-670.	7.2	24
38	On the role of precipitates in controlling microstructure and mechanical properties of Ag and Sn added 7075 alloys during artificial ageing. Materials Science & Engineering A: Structural Materials: Properties, Microstructure and Processing, 2018, 738, 399-411.	5.6	55
39	Deformation and annealing behaviour of dual phase TWIP steel from the perspective of residual stress, faults, microstructures and mechanical properties. Materials Science & amp; Engineering A: Structural Materials: Properties, Microstructure and Processing, 2018, 733, 43-58.	5.6	16
40	Application of analytical hierarchy process (AHP) for flood risk assessment: a case study in Malda district of West Bengal, India. Natural Hazards, 2018, 94, 349-368.	3.4	160
41	Quantitative approach on erosion hazard, vulnerability and risk assessment: case study of Muriganga–Saptamukhi interfluve, Sundarban, India. Natural Hazards, 2017, 87, 1709-1729.	3.4	19
42	Addressing the selectivity issue of cobalt doped zinc oxide thin film iso-butane sensors: Conductance transients and principal component analyses. Journal of Applied Physics, 2017, 122, .	2.5	14
43	Modeling the sensing characteristics of chemi-resistive thin film semi-conducting gas sensors. Physical Chemistry Chemical Physics, 2017, 19, 23431-23443.	2.8	41
44	Understanding on the selective carbon monoxide sensing characteristics of copper oxide-zinc oxide composite thin films. Sensors and Actuators B: Chemical, 2017, 253, 685-696.	7.8	26
45	Volatile organic compound sensing using copper oxide thin films: Addressing the cross sensitivity issue. Journal of Alloys and Compounds, 2017, 692, 108-118.	5.5	60
46	Vulnerability assessment through index modeling: a case study in Muriganga–Saptamukhi estuarine interfluve, Sundarban, India. Arabian Journal of Geosciences, 2017, 10, 1.	1.3	9
47	Process Form Responses of Shoreline Erosion Using Geo-Spatial Techniques: Case Study in Muriganga-Saptamukhi Interfluve, Sundarban. Earth Science India, 2017, 10, .	0.1	1
48	Total Extraction as a Treatment for Anaemia in a Patient of Glanzmann's Thrombasthenia with Chronic Gingival Bleed: Case Report. Journal of Clinical and Diagnostic Research JCDR, 2016, 10, ZD11-2.	0.8	3
49	Engineered spinel–perovskite composite sensor for selective carbon monoxide gas sensing. Sensors and Actuators B: Chemical, 2016, 225, 128-140.	7.8	32
50	Phase Formation Behavior and Hydrogen Sensing Characteristics of Iron Oxide Nano-Particles Synthesized by Modified Pechini Route. Materials Focus, 2016, 5, 119-122.	0.4	0
51	Selective hydrogen sensing by cobalt doped ZnO thin films: A study on carrier reversal conductivity. , 2015, , .		2
52	Understanding the anomalous conduction behavior in †n' type tungsten oxide thin film during hydrogen gas sensing: Kinetic analyses of conductance transients. Sensors and Actuators B: Chemical, 2015, 220, 949-957.	7.8	10
53	Hematite iron oxide nano-particles: facile synthesis and their chemi-resistive response towards hydrogen. Materials Research Express, 2015, 2, 055901.	1.6	10
54	′Sutureless′ transconjunctival approach for infraorbital rim fractures. Contemporary Clinical Dentistry, 2015, 6, 56.	0.7	3

#	Article	IF	CITATIONS
55	Accidental Ingestion of Removable Partial Denture, Leading to Tracheoesophageal Fistula. Journal of Maxillofacial and Oral Surgery, 0, , 1.	1.4	0
56	Consistent Level IIa Node as a Surgical Landmark for Identification of Spinal Accessory Nerve. Journal of Clinical and Diagnostic Research JCDR, 0, , .	0.8	0